NASA-TM-85809

NASA Technical Memorandum 85809

NASA-TM-85809 19840017859

Edge Analyzing Properties of Center/Surround Response Functions in Cybernetic Vision

Daniel J. Jobson

May 1984

National Aeronautics and
Space Administration

Langley Research Center
Hampton, Virginia 23665

DISPLAY 21/2/1

84N25927*#   ISSUE 16   PAGE 2484   CATEGORY 33   RPT#: NASA-TM-85809 NAS 1.15:85809   84/05/00   34 PAGES   UNCLASSIFIED DOCUMENT

UTTL: Edge analyzing properties of center/surround response functions in cybernetic vision

AUTH: A/JOBSON, D. J.

CORP: National Aeronautics and Space Administration. Langley Research Center, Hampton, Va.   AVAIL.NTIS   SAP: HC A03/MF A01

MAJS: /*CONTRAST/*CYBERNETICS/*EDGES/*HIGH RESOLUTION/*MAN MACHINE SYSTEMS/* PATTERN RECOGNITION

MINS: / COMPUTER VISION/ DECISION MAKING/ HUMAN FACTORS ENGINEERING/ IMAGE PROCESSING/ VISUAL PERCEPTION

ABA: Author

ABS: The ability of center/surround response functions to make explicit high resolution spatial information in optical images was investigated by performing convolutions of two dimensional response functions and image intensity functions (mainly edges). The center/surround function was found to have the unique property of separating edge contrast from shape variations and of providing a direct basis for determining contrast and subsequently shape of edges in images. Computationally simple measures of contrast and shape were constructed for potential use in cybernetic vision systems. For one class of response functions these measures were found to be reasonably resilient for a range of scan direction and displacements of

ENTER:

22   1   1 RN/NASA-TM-85794

EDGE ANALYZING PROPERTIES OF CENTER/SURROUND RESPONSE FUNCTIONS IN CYBERNETIC VISION

by Daniel J. Jobson

ABSTRACT

The ability of center/surround response functions to make explicit high resolution spatial information in optical images was investigated by performing convolutions of two dimensional response functions with image intensity functions (mainly edges). The center/surround function was found to have the unique property of separating edge contrast from shape variations and to provide a direct basis for determining contrast and subsequently shape of edges in images. Computationally simple measures of contrast and shape were constructed for potential use in cybernetic vision systems. For one class of response functions these measures were found to be reasonably resilient for a range of scan directions and displacements of the response functions relative to shaped edges. A pathological range of scan directions was also defined and methods for detecting and handling these cases were developed. The relationship of these results to natural vision is discussed speculatively.

INTRODUCTION

The ease with which animal organisms, including man, extract spatial information from the optical image and integrate this information into intelligent decision making and visually cued movement is remarkable. Much research in artificial vision has been stimulated by the characteristics of the biological sense of vision. Studies of biological vision have established the pervasive presence of receptive fields with opponent responses in the several stages of early visual processing and the primary sensitivity of these responses to contrast phenomena. Principal findings in artificial vision have been: 1) opponent responses are inherently edge enhancing as spatial bandpass filters, 2) edge detection can be accomplished by detecting zero crossings (Ref. 1, and 2), and 3) reflectance changes can be isolated from illumination variations by sampling with opponent response functions (Ref. 3). These results are general for both types of opponent response functions (circular and linear types). The only distinction made in these previous studies is the insensitivity of circularly symmetric responses to scan direction for straight edges.

A sharp distinction in two dimensions exists between the circular symmetry of retinal, lateral geniculate, and concentric cortex receptive fields and the linear character of the simple and complex neuron receptive fields in the cortex. Therefore, the two types of responses are explored in this paper to determine any other interesting properties of opponent response functions. Properties of the center/surround response function are of special interest for three reasons: 1) its position in the overall vision architecture as the first level of image sensing and processing, 2) its relationship to focal plane processing concepts in cybernetic vision, and 3) recent discoveries of its increasingly significant role in the primate visual cortex (see Appendix). The efficiency of natural vision in combination with the extraordinary slowness of neurological signaling rates and response times suggest the existence of additional characteristics of center/surround response function which may aid the spatial information extraction process and be useful in artificial vision systems. In order to investigate this possibility, two-dimensional models of opponent response functions are constructed and convolved with two-dimensional edge functions. Considerable emphasis is placed on circularly symmetric functions analogous to receptive fields in the retina and the first stages of visual processing in the brain.

METHODS

Models of opponent response functions have been based on various mathematical forms (difference of Gaussian Ref. 4; Laplacian, Ref. 1; Gaussian sine and Gaussian cosine, Ref. 5) and emphasized accurate modeling of the spatial response of the receptive field. For this investigation simplified "boxcar" response functions and edge functions (Fig. 1a and b) were used first as a convenient tool. The difference of Gaussian response (Fig. 2) function was selected to confirm the properties for a more accurate smoothly varying function. The variables of interest were the amplitude relationship of opposing components in the response function, edge contrast and shape, the scan direction of the convolution, and relative alignment of the response and shaped edge functions. These variables are summarized schematically in Fig. 1-3 with symbolic definitions of variables. The assumption was made that fundamental properties of the response functions based on circular and linear character of response functions would be preserved with "boxcar" functions. The discrete nature of digital forms of the response and edge functions is shown in Fig. 4 to illustrate a limitation of the model, i.e. circular symmetry is only approximate for the center/surround and shaped edges are composed of two approximately straight lines. Edge shape is modeled as convex or concave by the angle ϕ, being less than or greater than 180° respectively. Two "boxcar" response amplitude cases were investigated: 1) balanced center/surround ($R_+ = 1.0$, $R_- = -.135$) where no response to uniform image intensity occurs, and 2) imbalanced center/surround ($R_+ = 1.0$, $R_- = -.10$) which possesses attenuated response to uniform image intensities.

Likewise for the smoothly varying DOG function, both balanced and imbalanced cases were included. The DOG function used was:

$$R_{DOG}(x,y) = 3^{-(x_i^2+y_j^2)/\sigma_1^2} - Ce^{-(x_i^2+y_j^2)/\sigma_2^2} \tag{1}$$

For the balanced DOG $\sigma_1 = 2.5$, $\sigma_2 = 3.3$, and $C = .574$ while for the imbalanced case $C = .567$ with no change in σ_1, and σ_2. The balanced center/surround being analogous to lateral geniculate body receptive fields while the imbalanced one is more representative of retinal receptive fields. Highly accurate models of biological receptive fields response shapes and the relative or absolute amplitudes of opponent lobes were not constructed since the primary purpose of the investigation was to explore fundamental response properties which could be used in the design of cybernetic vision systems.

The convolutions were performed as discrete integral summations

$$s(x') = \sum_{j=1}^{m} \sum_{i=1}^{n} I\,(x_i - x', y_j)\, R(x_i, y_j)\ \Delta x_i \Delta y_j \tag{2}$$

in which Δx_i and Δy_j are assigned the value of unity since positions on image or response functions are discrete digital numbers. The convolution is intended to be analogous to the physical scanning of an image element across a receptive field by eye movement at microscopic scales.

CONVOLUTION RESULTS

Initial Results for Various Opponent Response and Image Functions

Convolutions were made for the balanced "boxcar" center/surround and linear symmetric and antisymmetric functions and several types of image functions with emphasis on edges though some checkerboard texture patterns (at or smaller than the scale of the response function) were included. Image functions were at full contrast (dark areas are zeros while light areas are unity, i.e. $\Delta I = 1$) except for one texture pattern where a much lower contrast ($\Delta I = 0.2$) was examined. Unlike the case for a single neuron's receptive field, negative signal amplitudes were allowed. These initial results are shown schematically in Fig. 5. The signals are not drawn to scale in terms of amplitude or relative spatial position but approximate "peak and valley" numerical magnitudes are indicated. The most interesting feature is the asymmetry which develops in the "bipolar" (positive to negative) signal amplitudes for shaped edges (corners with 90° or 270° angle in the example). Further, the asymmetry is in a positive direction for convex edge shapes and conversely in a negative direction for concave edge shapes. This suggests that edge shape may be directly related to a measure of signal amplitude asymmetry. This property of the center/surround is not shared by the linear opponent response functions and, of course, is not a property of the discrete image element by element response functions of television or detector array cameras.

Results for linear opponent response functions indicate the expected sensitivity to edge contrast and orientation and yield no clear cut approach to separating shape from orientation variations. Little difference in spatial information content of the signals can be discerned between the two linear opponent response functions. The phase difference in the signals (Ref. 6 and 7) is not apparent in the figure since the curves were not spatially registered but is obvious in correctly registered data. One curious difference is that the antisymmetric response function normally responds to edges with all positive signals or all negative signals depending on direction of convolution scan, edge amplitudes, and positive and negative response lobes relationships. Both positive and negative signals occur only for small scale textures (modeled as a checkerboard).

To further examine the ability of the center/surround to isolate edge shape information from edge contrast information, convolutions were carried out for the balanced and imbalanced center/surround for various edge shapes and contrasts.

<u>Balanced "Boxcar"Center/Surround</u> ($R_+ = 1.0$, $R_- = 0.135$)

Since the balanced center/surround response function has no response to uniform intensity fields, it produces convolution results that are most directly interpretable with respect to edge information. The straight edge-variable contrast case is shown in Fig. 6a while the constant contrast-variable shape case is presented in Fig. 6b. An example (Fig. 6c) of variable contrast-shaped edge ($\phi = 90°$) is given for completeness. The most noticeable feature of these curves is the presence of a steadily shifting "peak" point (S_+) and "valley" point (S_-) for all edges. The curves also suggest that the amplitude difference between the "peak" and "valley" points is a function of contrast and that this contrast information is preserved with reasonable accuracy for a wide variety of edge shapes. Likewise, the degree of asymmetry in positive versus negative signal "peaks" and "valleys" is suggested as a measure of edge angularity. Convenient mathematical forms are $\Delta S_- = S_+ - S_-$, and $\Delta S_+ = S_+ + S_-$. Therefore, ΔS_- and ΔS_+ will be investigated later as a measure of contrast and shape, respectively.

Imbalanced "Boxcar" Center/Surround ($R_+ = 1.0$, $R_- = -.10$)

The same edge functions were convolved with the imbalanced center/surround response function (Fig. 7). Similar trends to the balanced center/surround exist but with the addition of non-zero signal levels before and after an edge event which are related to the image intensity levels on either side of the edge. Unlike the balanced center/surround case, S_- and S_+ are not as obviously measures of contrast and shape, respectively.

For the cases shown thus far, the scan direction ($\phi = 0°$) was perpendicular to the straight edge or directed straight at the point of the corner for shaped edges. The geometrical center of the center/surround response function was aligned to point at the corner for shaped edges ($d = 0$). The more general case of other scan directions and displacements of the response center with respect to the corner point will be treated as resiliency tests for the measures of contrast and shape.

DOG Center/Surround

Convolutions for both balanced and imbalanced DOG response functions (Fig. 8 as an example) show the same trends with slight differences in the overall functional relationships. This result provides evidence for the generality of contrast and shape sensitivity based on the circular symmetry of the center/surround response function independent of the specific mathematical form of the function.

Measures of edge contrast and shape. From the preceding convolution results, the relationships of ΔS_- and ΔS_+ to contrast and shape were determined, for both balanced and imbalanced center/surround (Fig. 9 and 10). The relationships for both measures and both balanced and imbalanced "boxcar" center/surrounds are reasonably linear. Further, the independence of ΔS_- to shape variations and of ΔS_+ to contrast variations was tested and is plotted on both figures. The contrast measure was found to be largely independent of shape variations for both types of center/surround. The shape measure for the balanced center/surround was highly contrast dependent (family of shape curves for different contrasts). A different shape measure, $\Delta S_+/\Delta S_-$, for the balanced center/surround was found to be largely independent of contrast (Fig. 10b). For the imbalanced center/surround ΔS_+ and $\Delta S_+/\Delta S_-$ were both dependent on contrast. Even though no contrast independent measure of shape was found for this response function, determinations are possible after initial contrast determination via a look-up table representing the family of curves for ΔS_+. For the contrast and shape values tested, the errors in one variable due to wide variations in the other are given in Table 1. The same measures for the DOG functions (Fig. 11) exhibit very similar characteristics.

Tests for resiliency and pathological cases. The resiliency of the measures to more arbitrary convolution geometries was tested by performing additional convolutions in which scan direction and the relative position of the geometric center of the "boxcar" center/surround to the corner point of the shaped edge were varied (Fig. 3). Although significant errors are introduced for some cases of scan direction and response misalignment (Fig 10 and Table 2), sufficient accuracy is maintained over a wide enough range of cases for the measures to be considered for practical application in sampling and processing image data. Some types of errors tend to be offsetting and in some instances are systematic (nonrandom). Therefore, potential for error reduction exists.

Pathological cases do exist for a range of scan directions. These fall into two categories: 1) the scan direction runs along an edge ($\theta = 1/2\phi$, $180° - 1/2\phi$), or 2) crosses a shaped edge twice ($180° - 1/2\phi < \theta < 1/2\phi$) within too short a distance for the development of full amplitudes of ΔS_+ and ΔS_- for either edge event. Examples of these cases (Fig. 12) give some indication how these cases can be detected. Except for one case (imbalanced center surround, $\theta = 1/2\phi$, $180°-\frac{1}{2}\phi$) the existence of a pathological case is evident from the general character of convolution results. A three lobed $S(x')$ is produced by both response types for the double crossing of a shaped edge and indicates the presence of a shaped edge with indeterminant contrast and shape. For the balanced center/surround, a convolution scan directed along a straight edge is evident by the absence of either the pre-event or the post-event zero levels. The same convolution geometry for the imbalanced center/surround is entirely undetectable and yields ambiguous determinations of contrast and shape. In the example shown ($\Delta I = 0.5$, $\phi = 90°$) would produce a ΔI estimate of about 0.6 and a ϕ of 150°. This case can only be detected at the strategy level after multiple scans from different directions and decision making based on the consistency of results.

Use in Artificial Vision Systems

For the shape and contrast measures to form a part of an artificial vision system, center/surround sampling of either the image directly or image data after it has been sensed and converted to a train of electronic signals must be accomplished first. Computer hardware or software image data processing coupled with current image sensing technologies have been investigated as a part of zero crossing studies. Initial software operations on images with 512 pixels square required 3 hours to apply the center/surround operation and determine zero crossings. Subsequent hardware implementations reduced this time to 0.25 second for images with 128 pixels square (Ref. 8). The approach of sensing the optical image directly with an ensemble of center/surround response functions implemented in an electronic device has been analyzed (Ref. 9) and found to have advantages over purely digital processing approaches in terms of reduced aliasing and electronic noise as well as reduced data volume transmitted from sensor to a storage medium or digital computer. Such devices do not presently exist but a number of device concepts and technologies have potential for sampling an image with an ensemble of center/surround response functions. This latter approach is analogous to the integrated sensing and processing of the image by the retina.

Regardless of the technological approach used to sample an image with center/surround response functions, the contrast and shape measures would form a part of the initial stage of image processing. Strategies for the practical use of these measures are beyond the scope of this investigation and must be developed as a part of an overall vision system architecture. However, one specific strategy element can be defined to avoid the calculation of $\Delta S_+/\Delta S_-$ with its computationally undesirable arithmetic division and for shape determinations with the imbalanced center/surround where no contrast independent shape measure has been found. This involves forming a small lookup table of edge elements of equal contrast and performing shape determinations within each isocontrast group. The choice of either the balanced or the imbalanced center/surround response functions is dictated by the goals and requirements of subsequent higher level image processing with the main consideration being the retention of image intensity level information which is a characteristic of the imbalanced center/surround. The handling of ambiguities arising from pathological or high error cases must be accomplished primarily at the strategy level. Images could be scanned across an ensemble of response functions several times in rapid succession each from a different direction and with arbitrary starting positions. The consistency of classifying image elements into contrast and shape categories could then be tested with a majority rule decision for major inconsistencies while smaller discrepancies could be handled with some combination of averaging and majority rule. Iterative cross comparisons between contrast and shape determinations could reduce errors due to the weak interdependence of contrast and shape.

Relationship to Biological Vision

There is no direct anatomical or electrophysiological evidence that neurons in the eye or brain of higher animals analyze the spike frequencies received from neurons with center/surround receptive fields and determine edge shape and contrast at high spatial resolution. However, since the isolation of edge shape and contrast information seems to be a general image sampling property of center/surround response functions, a speculative discussion of biological vision is warranted.

Neurons of the retina, lateral geniculate, and the striate cortex possess concentric receptive fields which differ in two major respects from the response functions studied here. The color opponency of primates concentric fields is not included in this model. No negative signal amplitudes are transmitted by a single neuron (i.e. only inhibitory spike frequencies between the spontaneous firing rate and zero are transmitted) therefore, the shape and contrast measures could not be derived from a single neuron in general. Possibly the combination of one "on-center" and one "off-center" neuron together supply the same type of information as the center/surround response function. This has been suggested by Marr (Ref. 2) in relation to zero crossing determinations. Some anatomical evidence does exist for this (Ref. 10) but has been investigated for dual opponent color rather than spatial processing. Only x-type neurons should be compared to the simplified response functions since this class of neurons has been demonstrated to form a linear response system (satisfy requirements for convolution integral) at least for photopic light intensity levels well below saturation levels (Ref. 11). The circular symmetry of the center/surround response function appears to be fundamentally responsible for making edge shape and contrast information explicit. Therefore it is likely to be an intrinsic property of the center/surround receptive fields of at least x-type neurons in higher animals.

Aside from edge shape and contrast information (and attenuated intensity information for imbalanced center/surround), it is difficult to find any other purely spatial information (other than edge sharpness or focus and, of course, location in image) available in signals from center/surround response functions. This suggests the highly speculative idea that this is the primary high resolution spatial information carried through the biological vision system and is sufficient to form the basis of subsequent image processing in higher animals. The identical hypothesis for cybernetic vision is that high resolution edge shape and contrast information is a sufficient starting point for the spatial information extraction process leading ultimately to vision based artificial intelligence.

The idea that edge shape plays an important role in vision is illustrated at the perceptual level by Kanitza's (Ref. 12) subjective contour optical illusions and Attneave's (Ref. 13) information theoretic studies. In the illusions, a few key shaped edge segments together with a minimum of additional visual cues leads to visual perceptions of entire overlapped geometric figures for triangles, squares, circles, stripes and lines. Marr (Ref. 2) gives a Kanitza triangle without the additional visual cues and a strong impression of the complete figure is still created. These visual perceptions suggest that highly shaped edges (corners or edges with significant curvature) are more significant to object recognition than straight or slightly curved edges. The significance of highly shaped edge elements in defining object forms has also been illustrated dramatically by Attneave's demonstration that defining points of maximum curvature for an object's edges and connecting these points with straight lines is sufficient to produce a readily recognizable object (a sleeping cat in Attneave's example).

A hypothetical model for the early stages of retina-brain vision architecture of higher animals is beyond the scope of this study however an interesting complementary relationship between receptive fields with circular and linear character is evident. Center/surround receptive fields are capable of isolating edge contrast and shape information. On the other hand, linear opponent receptive fields are sensitive to variations in these quantities together with orientation (and a coarser scale than the retinal center/surrounds at least in one dimension) but lack the ability to distinguish between several signal variations due to the different variables. Therefore a hypothetical complementary architecture is postulated with center/surround receptive fields supplying edge contrast and shape determination which then allow simple cortical neurons to supply spatial information from which edge orientations and extent can be extracted.

CONCLUSIONS

Center/surround response functions as distinguished from other opponent image sampling functions have the ability to separate contrast and shape information for edges in the optical image. Computational measures for contrast and shape were constructed and tested for both balanced and imbalanced center/surrounds. Direct determinations of contrast were possible in both cases. A contrast independent shape measure was developed for the balanced center/surround while a look-up table approach was suggested for shape determinations from an imbalanced center/surround. The residual weak interdependence of contrast and shape measures was quantified, and the resiliency of the measures to arbitrary scan angles and displacements was investigated. For the cases examined the contrast and shape measures are sufficiently accurate and resilient to be considered for practical application in image sampling and processing. Pathological exceptions were found for scan geometries running along an edge or double crossing a shaped edge. The application of these results to artificial vision systems was discussed as well as the hypothetical relationship to biological vision.

APPENDIX

Recent Discovery of a Concentric Receptive Field Visual Subsystem in Primate Visual Cortex

The concentric receptive field has been known to be the dominant type in the retina and lateral geniculate body in higher animals. In addition, neurons with this type of receptive field were known to exist in layer 4 of the striate cortex. Recently, this type neuron has been found to occur in large numbers in layer 4C of the primate striate cortex, and a further major network of concentric field neurons has been discovered in the primate striate cortex (Ref. 14). This newly discovered network has been found to be a major extensive subsystem of the striate cortex contributing to most vertical layers of Area 17 and forming periodic columns horizontally (Ref. 15). Most recently this new network has been traced further to Area 18 cortex and forms a subsystem of layers alternating with orientation projection layers from Area 17 (Ref. 16). This new visual subsystem is not simply a relay system since receptive field properties differ markedly from the subcortical concentric fields and therefore appears to form an image processing subsystem in tandem with the other orientation sensitive subsystem.

REFERENCES

1. Marr, D., Hildreth, E., Theory of Edge Detection, Proc. R. Soc. Lond. B 207, 187-217 (1980).

2. Marr, D., Vision, San Francisco, W. H. Freeman and Company, 1982.

3. Horn, B. K. P., Determining Lightness from an Image, Computer Graphics and Image Processing, 3, 277-299 (1974).

4. Wilson, H. R., Bergen, J. R., A Four Mechanism Model for Threshold Spatial Vision, Vision Research 19, 19-32 (1979).

5. Marcelja, S., Mathematical Description of the Responses of Simple Cortical Cells, J. Opt. Soc. Am. 70, 1297-1300 (1980).

6. Pollen, D. A., Ronner, S. F., Phase Relationships Between Adjacent Simple Cells in the Visual Cortex, Science 212 (1981).

7. Kulikowski, J. J., Marcelja, S., Bishop, P. O., Theory of Spatial Position and Spatial Frequency Relations in the Receptive Field of Simple Cell in the Visual Cortex, Biol. Cybern. 43, 187-198 (1982).

8. Brady, M., Computational Approaches to Image Understanding Computing Surveys 14, 1 3-71 (1982).

9. Huck, F. O. et al, Image-Plane Processing of Visual Information, Applied Optics (to be published).

10. Michael, C. R., Color Vision Mechanisms in Monkey Striate Cortex; Dual-Opponent Cells with Concentric Receptive Fields, J. Neurophysiol., 41, 3, 572-588 (1978).

11. Levick, W. R., Receptive Fields of Retinal Ganglion Cells. In: Handbook of Sensory Physiology, Vol. VII/2, pp. 532-566., Fuertes, M. M. G. F. ed: Berlin, Heidelberg, New York, Springer, 1972.

12. Coren, S., Subjective contours and apparent depth, Psychol. Rev., 359-67 (1972).

13. Attneave, F., Some Informational Aspects of Visual Perception, Psychol. Rev. 61, 183-193 (1954).

14. Hubel, D. H., Exploration of The Primary Visual Cortex, 1955-78, Nature, 299, 515-524 (October 1982).

15. Livingstone, M. S.; and Hubel, D. H., Thalamic Inputs to Cytochrome Oxidase-Rich Regions in Monkey Visual Cortex, Proc. Natl. Acad. Sci., 79, 6098-6101 (October 1982).

16. Livingstone, M. S.; and Hubel, D. H., Specificity of Cortico-Cortical Connections in Monkey Visual System, Nature, 304, 531-534 (August 11, 1983).

TABLE 1

ERRORS DUE TO WEAK INTERDEPENDENCE OF EDGE CONTRAST AND SHAPE

	Shape Angle, ϕ	ΔS_-	Estimated ΔI	Difference Error	% Error	% of Full Range (1.0)
Balanced Center/Surround	37°, 323°	7.74, 7.74	0.57	+.07	+14	+7
	90, 270	7.51, 7.51	.55	+.05	+10	+5
	180	6.80	.50	0	0	0
	127, 233	6.90, 6.90	.51	+.01	+ 2	+1
Imbalanced Center/Surround	37, 323	8.45, 8.45	.545	+.045	+ 9	+4.5
	90, 270	8.25, 8.25	.535	+.035	+ 7	+3.5
	180	7.8	.50	0	0	0
	127, 233	7.7, 7.7	.495	-.005	- 1	- .5

a) Contrast Measure-Shape Variations ($\Delta I = 0.5$)

	Contrast	$\Delta S_+/\Delta S_-$	ϕ Estimated (by line)	Difference Error	% Error	% of Full Range (360°)
Balanced Center/Surround	0.2	.653	279°	+9°	+3.3	+2.5
	0.5	.626	275	+5	+1.9	+1.4
(ϕ = 270°)	1.0	.619	274	+4	+1.5	+1.1

b) Shape Measure-Contrast Variations

TABLE 2

ERRORS DUE TO SCAN DISPLACEMENT, d, AND DIRECTION, θ

	d	θ	Estimated ΔI	ΔI Error	Estimated φ	φ Error
Balanced Center/Surround (ΔI=0.5, φ = 90°)	0	0°	.55	+.05	90°	0°
	1	0	.49	-.01	95	+ 5
	2	0	.48	-.02	122	+32
	0	15	.51	+.01	92	+ 2
Imbalanced Center/Surround (ΔI=0.5, φ = 90°)	0	0	.52	+.02	78	-12
	1	0	.49	-.01	95	+ 5
	2	0	.47	-.03	122	+32
	0	15	.47	-.03	112	+22
	1	15	.535	+.035	103	+13
	2	15	.525	+.025	95	+ 5
	0	20	.42	-.08	133	+43
	1	20	.51	+.01	98	+ 8
	2	20	.525	+.025	95	+ 5

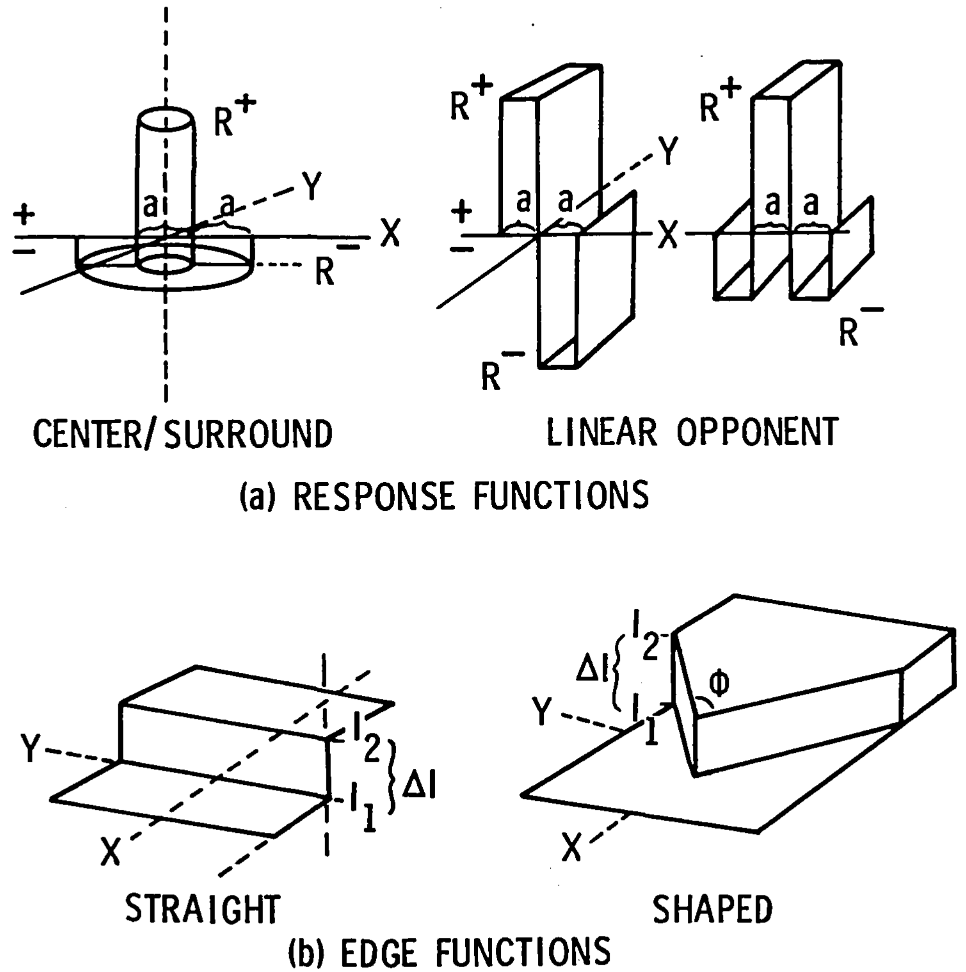

Figure 1.- "Boxcar" response and edge functions

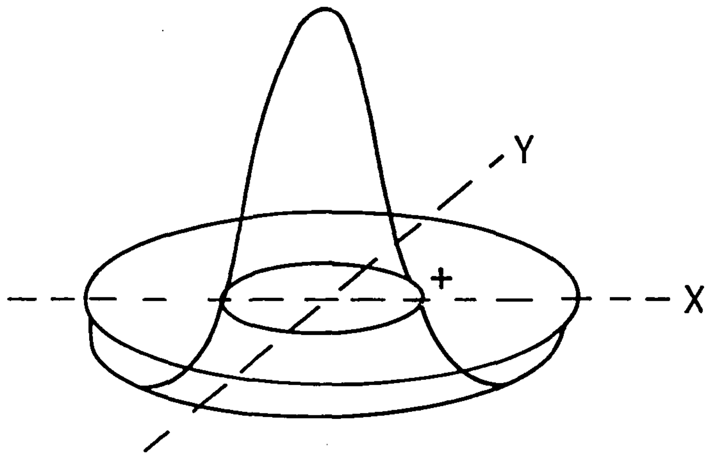

Figure 2.- Difference of Gaussian (DOG) response function (σ_1 = 2.5, σ_2 = 3.3)

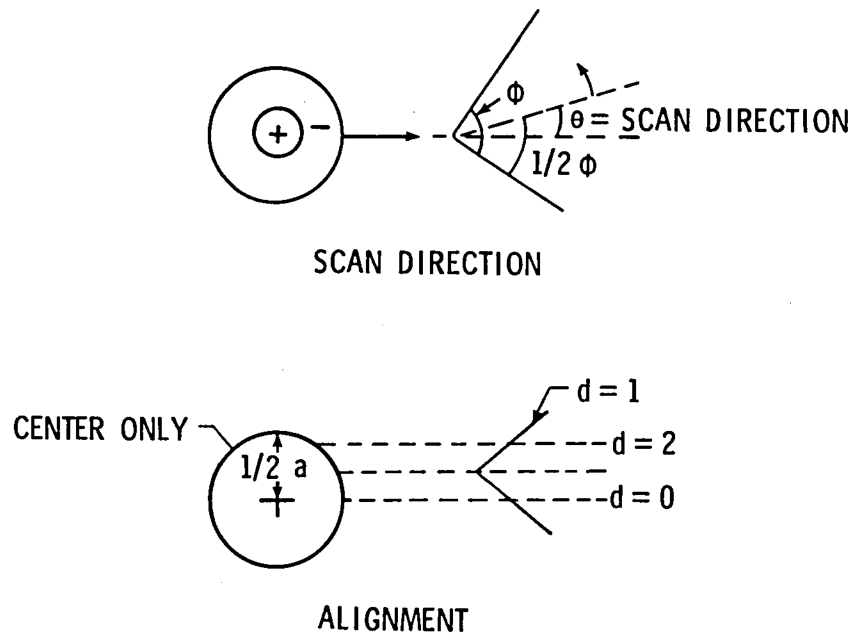

Figure 3.- Convolution geometries for shaped edges

					-.135	-.135	-.135	-.135	-.135					
			-.135	-.135	-.135	-.135	-.135	-.135	-.135	-.135	-.135			
		-.135	-.135	-.135	-.135	-.135	-.135	-.135	-.135	-.135	-.135	-.135		
	-.135	-.135	-.135	-.135	-.135	-.135	-.135	-.135	-.135	-.135	-.135	-.135	-.135	
	-.135	-.135	-.135	-.135	-.135	-.135	-.135	-.135	-.135	-.135	-.135	-.135	-.135	
-.135	-.135	-.135	-.135	-.135	-.135	1.00	1.00	1.00	-.135	-.135	-.135	-.135	-.135	-.135
-.135	-.135	-.135	-.135	-.135	1.00	1.00	1.00	1.00	1.00	-.135	-.135	-.135	-.135	-.135
-.135	-.135	-.135	-.135	-.135	1.00	1.00	1.00	1.00	1.00	-.135	-.135	-.135	-.135	-.135
-.135	-.135	-.135	-.135	-.135	1.00	1.00	1.00	1.00	1.00	-.135	-.135	-.135	-.135	-.135
-.135	-.135	-.135	-.135	-.135	-.135	1.00	1.00	1.00	-.135	-.135	-.135	-.135	-.135	-.135
	-.135	-.135	-.135	-.135	-.135	-.135	-.135	-.135	-.135	-.135	-.135	-.135	-.135	
	-.135	-.135	-.135	-.135	-.135	-.135	-.135	-.135	-.135	-.135	-.135	-.135		
		-.135	-.135	-.135	-.135	-.135	-.135	-.135	-.135	-.135	-.135	-.135		
			-.135	-.135	-.135	-.135	-.135	-.135	-.135	-.135	-.135			
					-.135	-.135	-.135	-.135	-.135					

A) Balanced Center/Surround

Figure 4.- Examples of Digital Forms of Response and Edge Functions

.50	.50	.50	.50	.50	.50	.50	.50	.50	.50	.50
.50	.50	.50	.50	.50	.50	.50	.50	.50	.50	.50
.50	.50	.50	.50	.50	.50	.50	.50	.50	.50	1.00
.50	.50	.50	.50	.50	.50	.50	.50	.50	1.00	1.00
.50	.50	.50	.50	.50	.50	.50	.50	1.00	1.00	1.00
.50	.50	.50	.50	.50	.50	.50	1.00	1.00	1.00	1.00
.50	.50	.50	.50	.50	.50	1.00	1.00	1.00	1.00	1.00
.50	.50	.50	.50	.50	1.00	1.00	1.00	1.00	1.00	1.00
.50	.50	.50	.50	1.00	1.00	1.00	1.00	1.00	1.00	1.00
.50	.50	.50	1.00	1.00	1.00	1.00	1.00	1.00	1.00	1.00
.50	.50	1.00	1.00	1.00	1.00	1.00	1.00	1.00	1.00	1.00
.50	1.00	1.00	1.00	1.00	1.00	1.00	1.00	1.00	1.00	1.00
.50	.50	1.00	1.00	1.00	1.00	1.00	1.00	1.00	1.00	1.00
.50	.50	.50	1.00	1.00	1.00	1.00	1.00	1.00	1.00	1.00
.50	.50	.50	.50	1.00	1.00	1.00	1.00	1.00	1.00	1.00
.50	.50	.50	.50	.50	1.00	1.00	1.00	1.00	1.00	1.00
.50	.50	.50	.50	.50	.50	1.00	1.00	1.00	1.00	1.00
.50	.50	.50	.50	.50	.50	.50	1.00	1.00	1.00	1.00
.50	.50	.50	.50	.50	.50	.50	.50	1.00	1.00	1.00
.50	.50	.50	.50	.50	.50	.50	.50	.50	1.00	1.00
.50	.50	.50	.50	.50	.50	.50	.50	.50	.50	1.00

B) Edge Function (ϕ = 90°)

Figure 4.- Examples of Digital Forms of Response and Edge Functions (Continued)

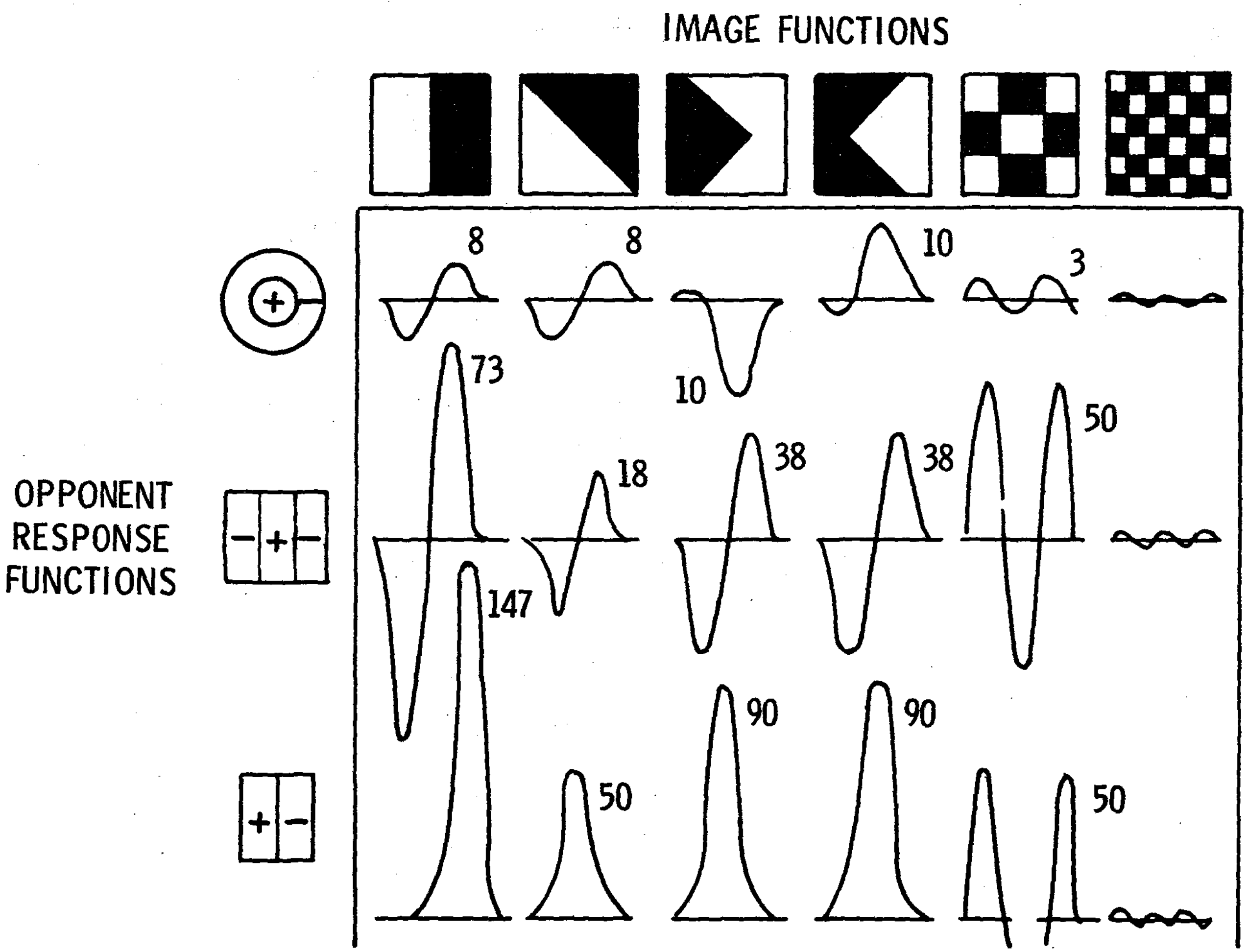

Figure 5.- Initial results

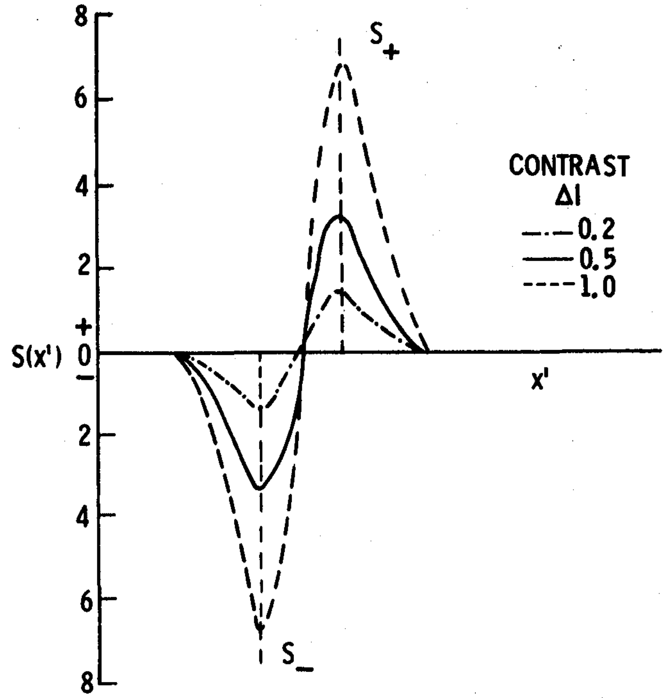

a) Contrast variations (ϕ = 180^{o})

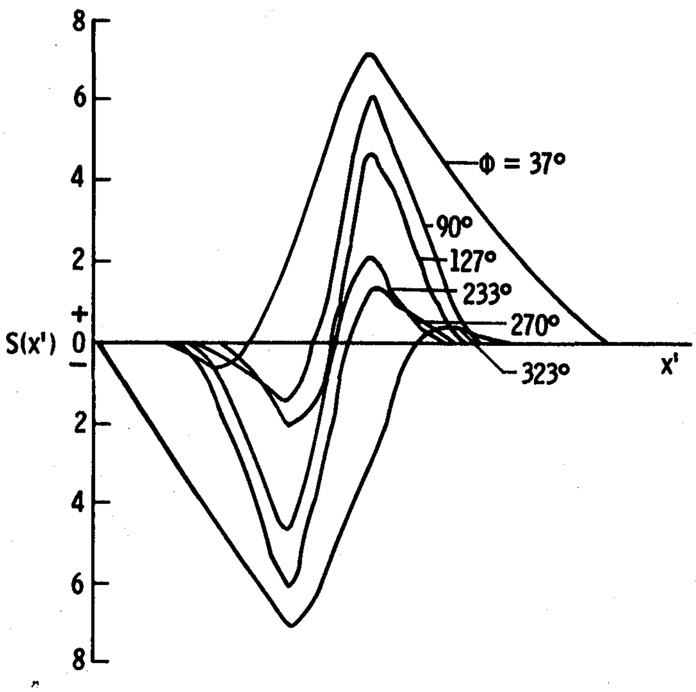

b) Shape variations (ΔI = 0.5)

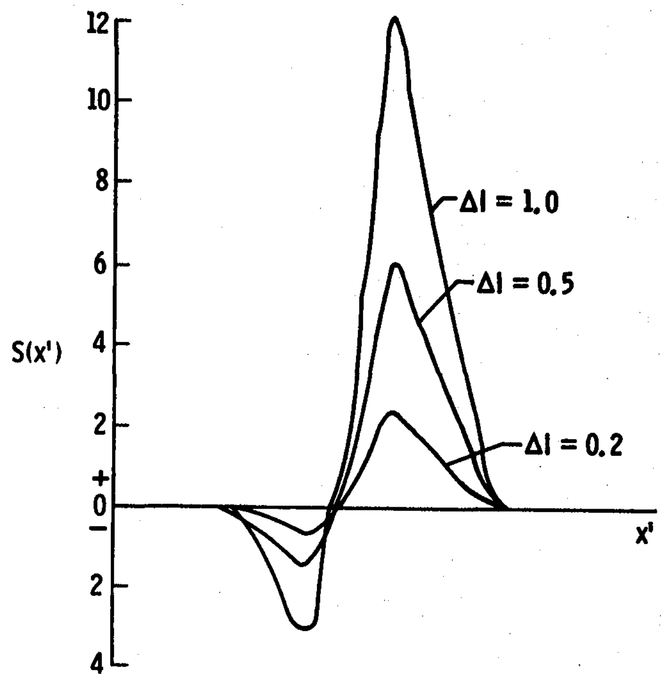

c) Contrast variations (ϕ = 90^{o})

Figure 6.- Convolution results: Balanced c/s

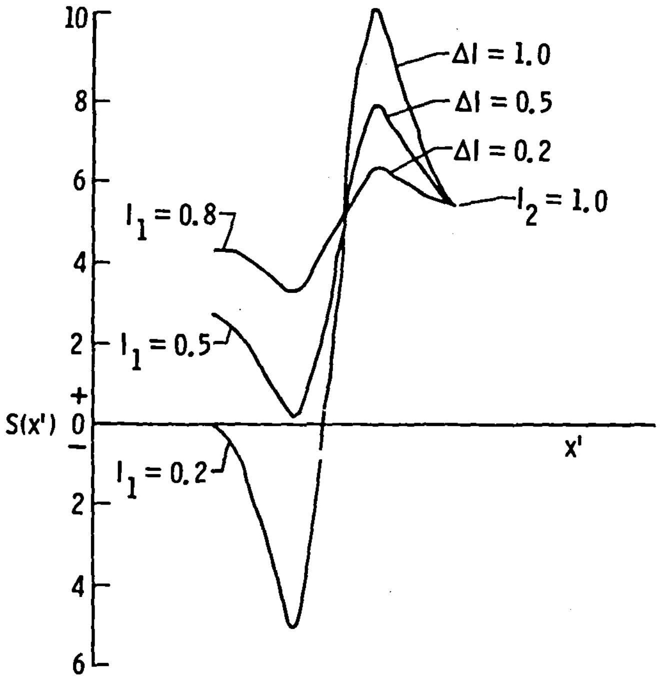

a) Contrast variations (ϕ = 180°)

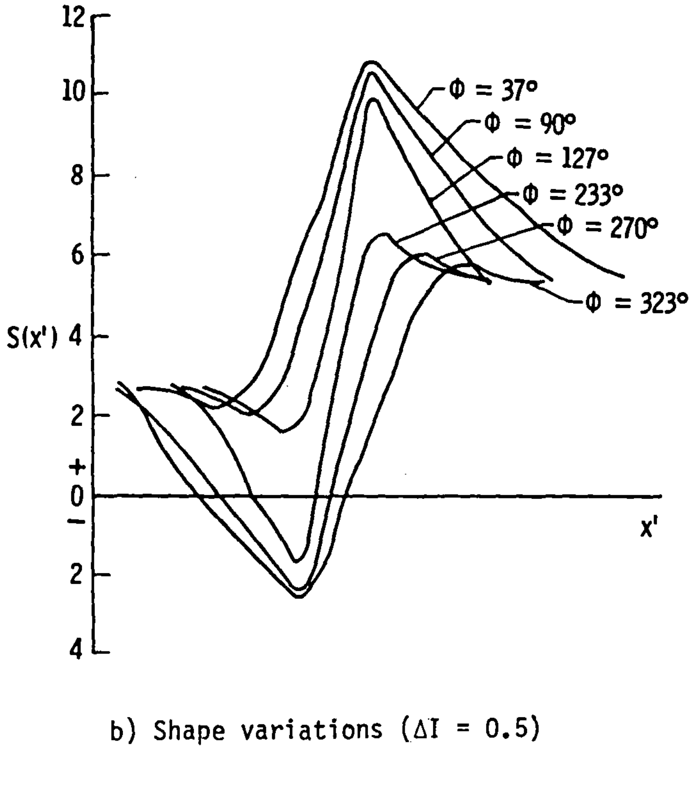

b) Shape variations (ΔI = 0.5)

Figure 7.- Convolution results: Imbalanced c/s

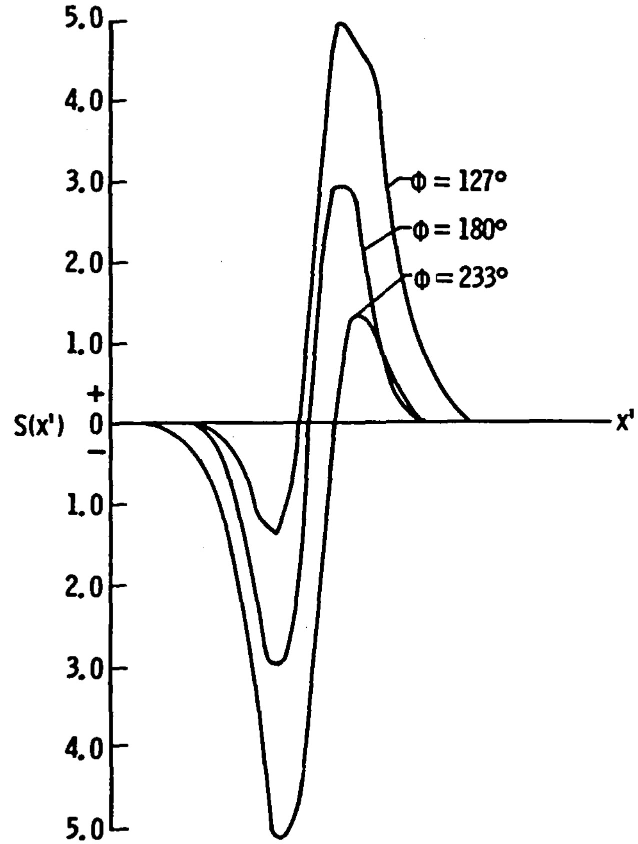

Figure 8.- Convolution results: Example for balanced DOG function ($\Delta I = 0.5$)

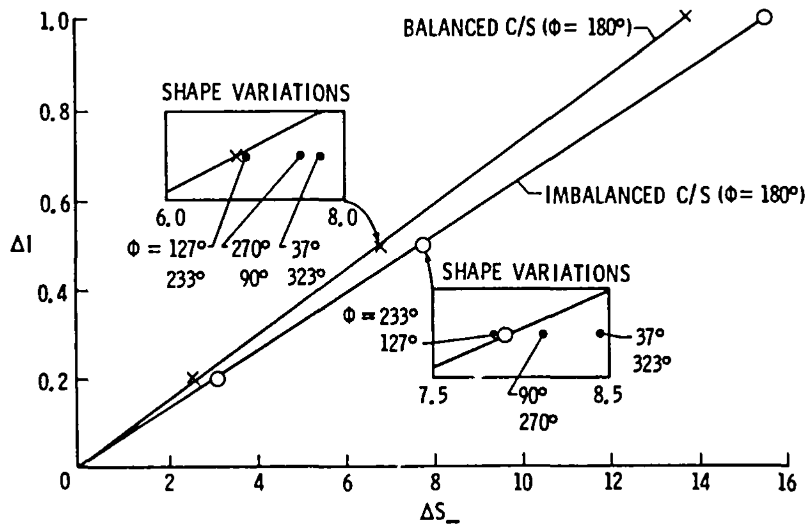

a) Contrast measure, ΔS_{-}

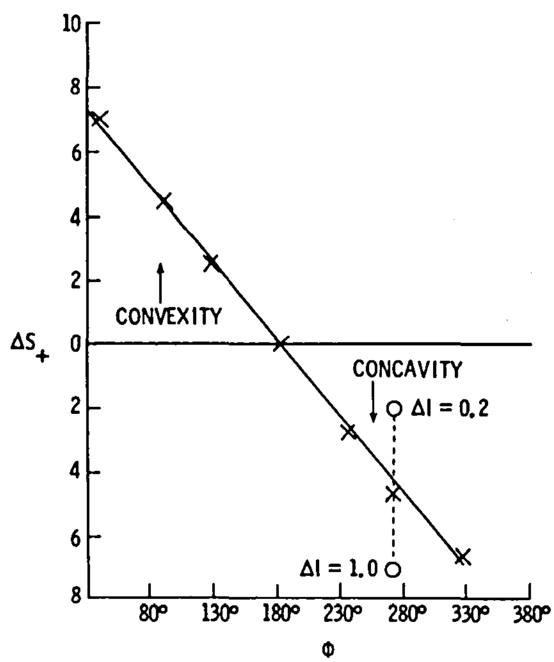

b) Shape measure, ΔS_{+}: Balanced c/s (contrast dependent)

Figure 9.- Measures of contrast and shape for c/s

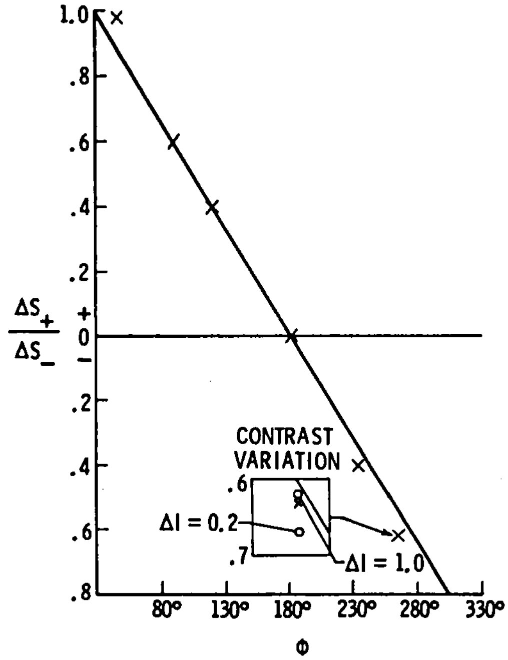

c) Shape measure, $\Delta S_+/\Delta S_-$: Balanced c/s (contrast independent)

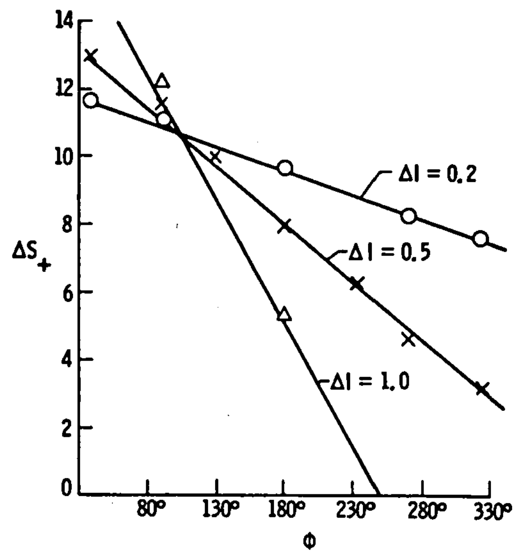

d) Shape measure, ΔS_+: Imbalanced c/s (contrast dependent)

Figure 9 (cont'd).

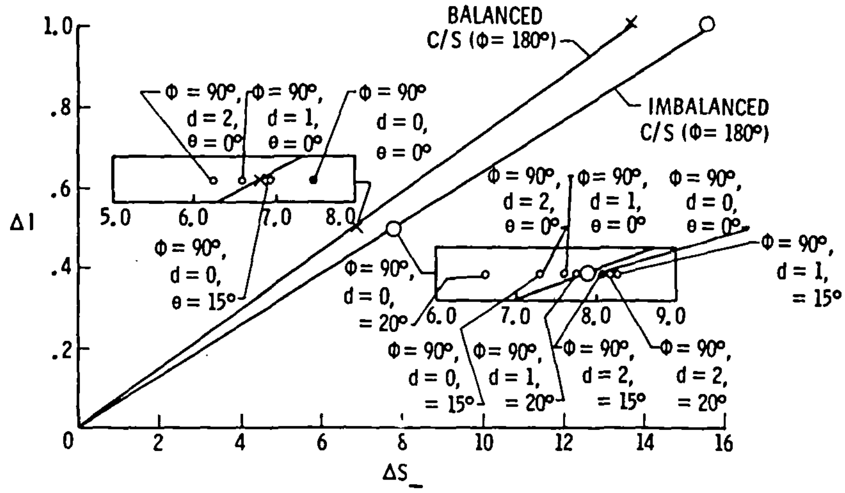

a) Contrast measure, ΔS_

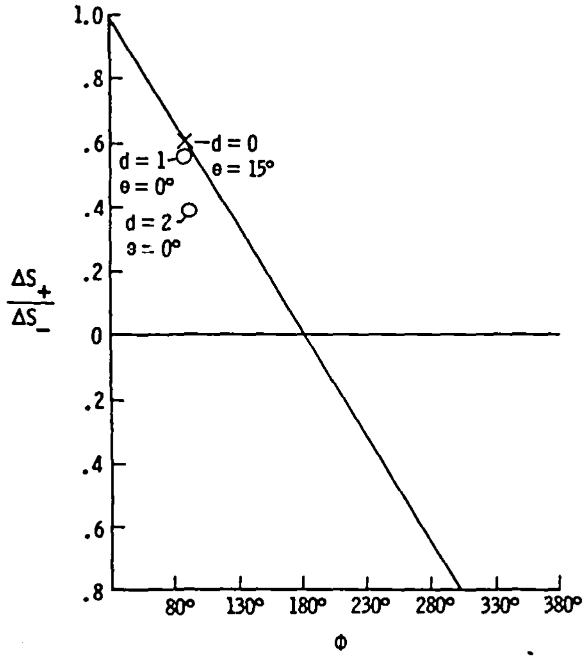

b) Shape measure, $\Delta S_+/\Delta S_-$: Balanced c/s

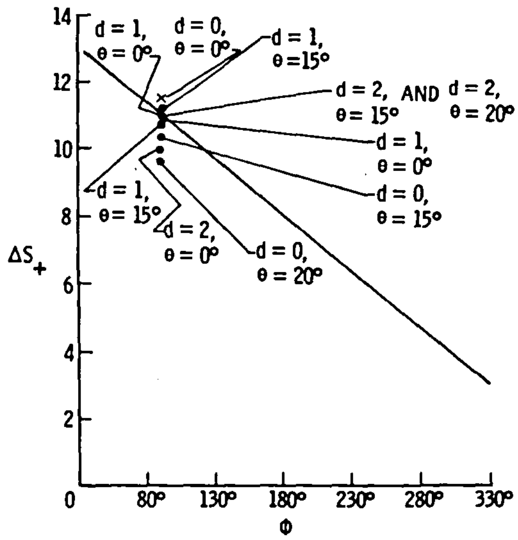

c) Shape measure, ΔS_+: Imbalanced c/s

Figure 10.- Resiliency of measures to response displacement, d, and scan direction, θ

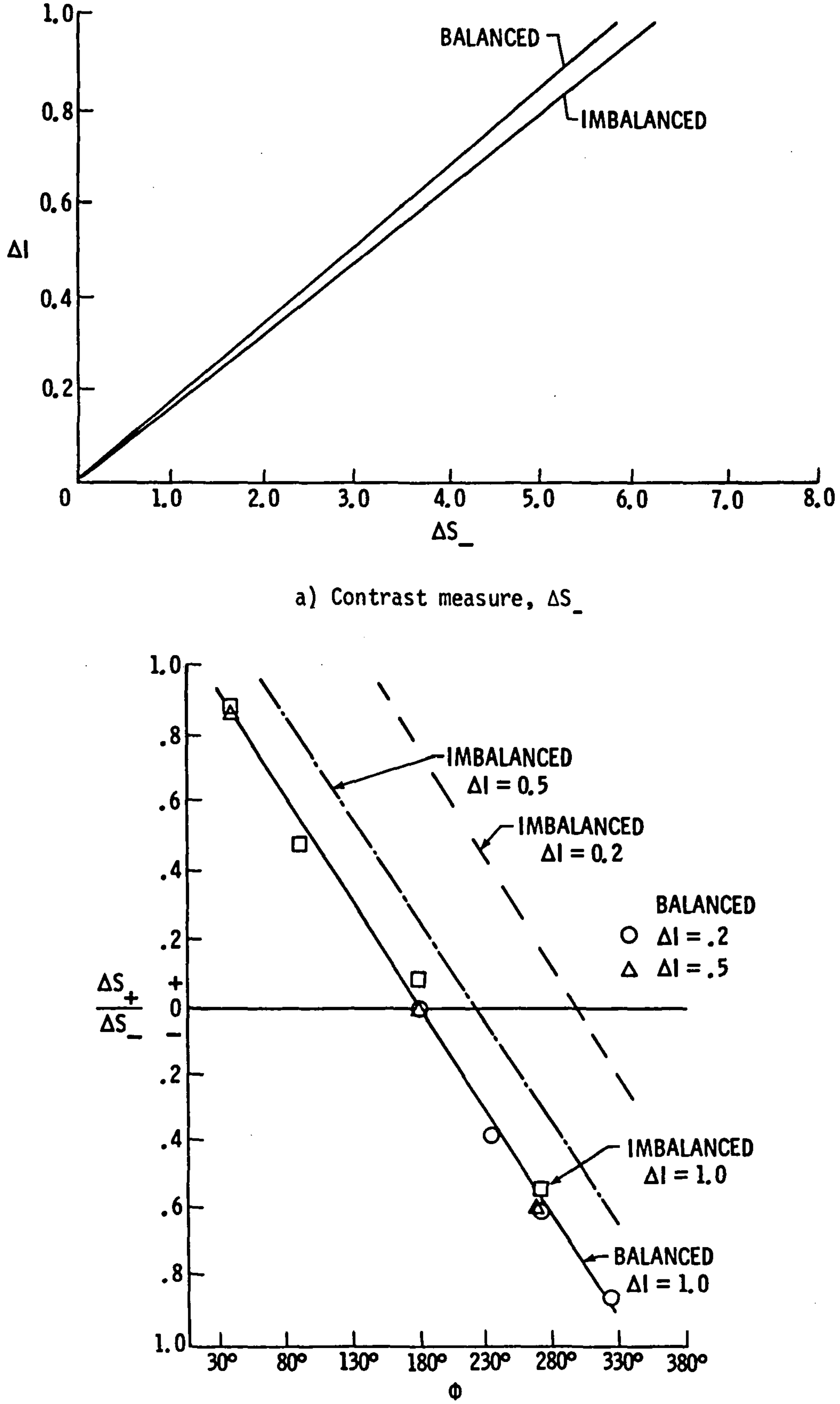

a) Contrast measure, ΔS_-

b) Shape measure, $\Delta S_+/\Delta S_-$

Figure 11.- Contrast and shape measures for DOG functions

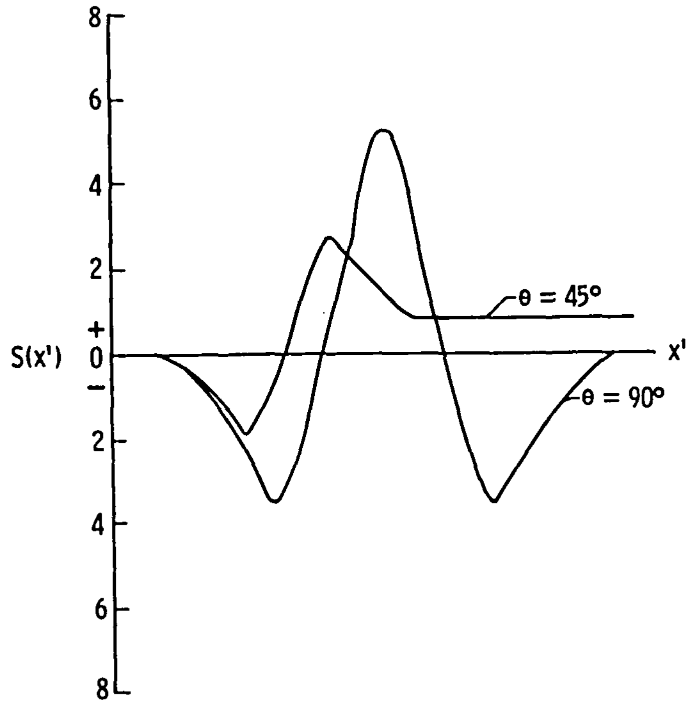

a) Balanced c/s ($\Delta I = 0.5$, $\phi = 90^0$)

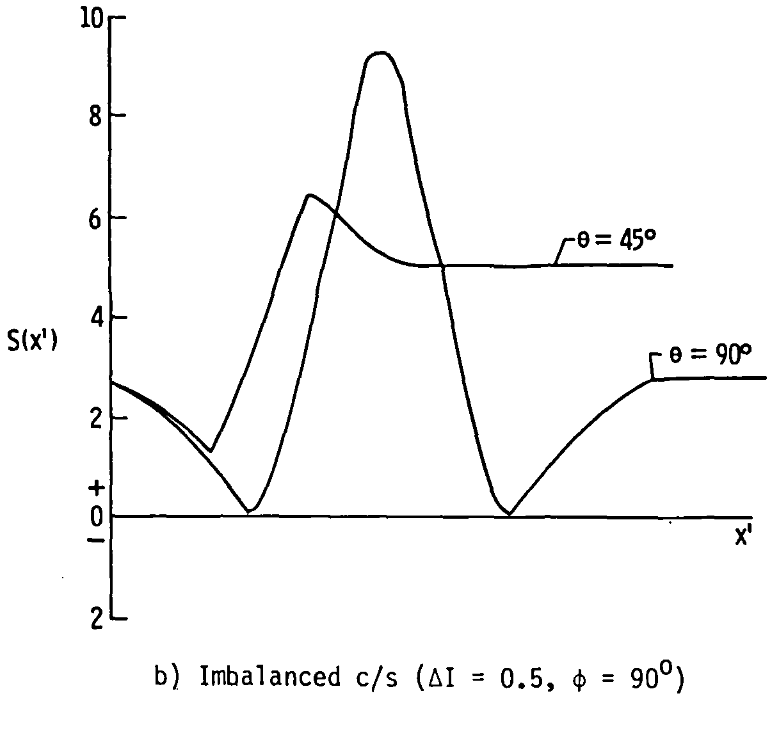

b) Imbalanced c/s ($\Delta I = 0.5$, $\phi = 90^0$)

Figure 12.- Pathological examples of scan direction, θ, for shaped edges

1. Report No.	2. Government Accession No.	3. Recipient's Catalog No.
NASA TM-85809		

4. Title and Subtitle	5. Report Date
Edge Analyzing Properties of Center/Surround Response Functions in Cybernetic Vision	May 1984
	6. Performing Organization Code 307-04-02-05
7. Author(s) Daniel J. Jobson	8. Performing Organization Report No.
	10. Work Unit No.
9. Performing Organization Name and Address NASA Langley Research Center Hampton, Virginia 23665	11. Contract or Grant No.
	13. Type of Report and Period Covered Technical Memorandum
12. Sponsoring Agency Name and Address National Aeronautics and Space Administration Washington, D.C. 20546	14. Sponsoring Agency Code

15. Supplementary Notes

16. Abstract

The ability of center/surround response functions to make explicit high resolution spatial information in optical images was investigated by performing convolutions of two dimensional response functions and image intensity functions (mainly edges). The center/surround function was found to have the unique property of separating edge contrast from shape variations and of providing a direct basis for determining contrast and subsequently shape of edges in images. Computationally simple measures of contrast and shape were constructed for potential use in cybernetic vision systems. For one class of response functions these measures were found to be reasonably resilient for a range of scan directions and displacements of the response functions relative to shaped edges. A pathological range of scan directions was also defined and methods for detecting and handling these cases were developed. The relationship of these results to biological vision is discussed speculatively.

17. Key Words (Suggested by Author(s))	18. Distribution Statement
Object Recognition, Cybernetic Vision, Center/Surround Response, Edge Analysis in Images	Unclassified - Unlimited Subject Category 33

19. Security Classif. (of this report)	20. Security Classif. (of this page)	21. No. of Pages	22. Price
Unclassified	Unclassified	33	A03